Available online at www.sciencedirect.com
SCIENCE DIRECT
Geochimica et Cosmochimica Acta 70 (2006) 2577–2590
Geochimica
www.elsevier.com/locate/gca

Influence of glass composition and alteration solution on leached silicate glass structure: A solid-state NMR investigation

Frédéric Angeli [a,*], Marina Gaillard [b], Patrick Jollivet [a], Thibault Charpentier [b]

[a] *Laboratoire d'Étude du Comportement à Long Terme, CEA Valrhô, 30207 Bagnols-sur-Cèze Cedex, France*
[b] *Laboratoire de Structure de Dynamique par Résonance Magnétique, CEA Saclay, 91191 Gif-sur-Yvette Cedex, France*

Received 9 September 2005; accepted in revised form 27 February 2006

Abstract

A multinuclear solid-state NMR investigation of the structure of the amorphous alteration products (so called gels) that form during the aqueous alteration of silicate glasses is reported. The studied glass compositions are of increasing complexity, with addition of aluminum, calcium, and zirconium to a sodium borosilicate glass. Two series of gels were obtained, in acidic and in basic solutions, and were analyzed using ^{1}H, ^{29}Si, and ^{27}Al MAS NMR spectroscopy. Advanced NMR techniques have been employed such as ^{1}H–^{29}Si and ^{1}H–^{27}Al cross-polarization (CP) MAS NMR, ^{1}H double quantum (DQ) MAS NMR and ^{27}Al multiple quantum (MQ) MAS NMR. Under acidic conditions, ^{29}Si CP MAS NMR data show that the repolymerized silicate networks have similar configuration. Zirconium as a second nearest neighbor increases the ^{29}Si isotropic chemical shift. The gel porosity is influenced by the pristine glass composition, modifying the silicon–proton interactions. From ^{1}H DQ and ^{1}H–^{29}Si CP MAS NMR experiments, it was possible to discriminate between silanol groups (isolated or not) and physisorbed molecular water near $Si(Q^2)$, $Si(Q^3)$, and $Si(Q^4)$ sites, as well as to gain insight into the hydrogen-bonding interaction and the mobility of the proton species. These experiments were also carried out on heated samples (180 °C) to evidence hydrogen bonds between hydroxyl groups on molecular water. Alteration in basic media resulted in a gel structure that is more dependent on the initial glass composition. ^{27}Al MQMAS NMR data revealed an exchange of charge compensating cations of the $[AlO_4]^-$ groups during glass alteration. ^{1}H–^{27}Al CP MAS NMR data provide information about the proximities of these two nuclei and two aluminum environments have been distinguished. The availability of these new structural data should provide a better understanding of the impact of glass composition on the gel structure depending on the nature of the alteration solution.

1. Introduction

Precise structural knowledge of the layer that develops on the surface of the glass during its aqueous alteration can be extremely useful for many applications, notably to describe the glass behavior and its properties depending on its environment. When the glass is leached, an alteration film commonly named "gel" forms on the glass surface. Its properties are of particular importance for long-term behavior studies of radioactive waste containment glass after it comes into contact with groundwater in a geological disposal. The gel that forms on the French high-level waste R7T7 glass exhibits diffusion properties that significantly diminish the glass alteration rate (Delage et al., 1992; Gin, 2000; Blet et al., 2002). It is also characterized by radionuclide retention properties, particularly for the transition metals, rare earth elements and actinides (Ménard et al., 1998). Both of these properties could be directly influenced by the gel structure, which is highly dependent on the alteration conditions such as pH. The structural evolution of the glass during leaching must therefore be finely characterized to better understand the possible impact of the structure of the gel on its aqueous reactivity and long-term properties. Given the complexity of the industrial glass, which comprises about 30 chemical elements (Advocat et al., 2001), it is preferable to investigate simplified glass compositions to determine the influence of the most representative elements. We propose in this

* Corresponding author. Fax: +33 4 66 79 66 20.
E-mail address: frederic.angeli@cea.fr (F. Angeli).

0016-7037/$ - see front matter © 2006 Elsevier Inc. All rights reserved.
doi:10.1016/j.gca.2006.02.023

study to investigate the potential of high-resolution solid-state NMR for probing the glass evolution during alteration (transformation into gel).

Most nuclear magnetic resonance (NMR) characterizations of the structural interaction between glass and water have been carried out on hydrated glass samples fabricated by quenching the hydrous melts at high pressure and temperature for investigations of rocks and magmas in the earth sciences (Kohn et al., 1992). Their physical and chemical properties can be better understood using structural characterizations, for example to determine whether the presence of water depolymerizes the glass network. Although this is still a subject of discussion (Zeng et al., 2000; Padro et al., 2003), these studies have extended our knowledge concerning proton sites using various NMR techniques (Kümmerlen et al., 1992; Schaller and Sebald, 1995; Robert et al., 2001; Ai et al., 2004; Cody et al., 2005). Hydroxyl groups and molecular water are routinely observed in hydrated aluminosilicates such as albite (Kohn et al., 1989a) with ^{1}H chemical shifts approximately ranged from 0 to 20 ppm. The possibility of selectively probing surface silicon atoms via the protons has been used to characterize the hydrated silica surface (Maciel and Sindorf, 1980; Chuang et al., 1993; Liu and Maciel, 1996; Chuang and Maciel, 1997; Ai et al., 2002, 2004; El Rassy and Pierre, 2005; Hu et al., 2005).

However, the mechanisms that occur during aqueous alteration of glass can be different from those observed with quenched hydrated glass or of silica gels. Literature on the structure of alteration gels is much less abundant. Information about the concentration of silanol surface complexes versus pH was obtained by ^{29}Si cross-polarization in media containing alkalis (Carroll et al., 2002), but the first structural study of altered glass samples by NMR was carried out by Bunker et al. (1988) on sodium borosilicate glasses leached at various pH values. The authors pointed out the transformation of the non-bridging oxygen atoms into silanol sites that reacted to form siloxane bonds. This repolymerization was observed regardless of the nature of the solution (although it was greater in acidic media), but the gel morphology was different. The same repolymerization was observed by ^{17}O MQMAS NMR on the alteration gel of a sodium aluminoborosilicate glass, which showed the restructuring of a boron-depleted aluminosilicate gel during alteration by $H_2{}^{17}O$ (Angeli et al., 2001).

In this work, we investigate the structure of the alteration gels formed from simple glasses containing oxides found in many natural and industrial glasses. Our purpose is to determine how the gel structure can be influenced by the alteration solution and the glass composition. Al, Ca, and then Zr were progressively added to a sodium borosilicate glass while maintaining the same molar proportions as in the SON68 glass (Advocat et al., 2001). The glass samples were then leached in acidic (pH 1) or basic (pH 9) solutions. The local environments of proton, silicon, and aluminum atoms were characterized by ^{1}H, ^{29}Si, ^{27}Al MAS NMR, ^{1}H DQ MAS NMR, and ^{27}Al MQMAS NMR. ^{1}H NMR was used to probe the surface of the alteration gel. In order to explore protonated environments, we performed ^{1}H–^{29}Si and ^{1}H–^{27}Al double resonance experiments: CPMAS and heteronuclear correlation (HETCOR) spectroscopy. Some gel samples were then heated to 180 °C to better identify the various proton resonances, particularly hydroxyl groups whose isotropic chemical shift in strongly influenced by the presence and the strength of hydrogen bonds with molecular water.

2. Experimental procedure

2.1. Glass compositions

All glass samples had the same B_2O_3/SiO_2 and Na_2O/SiO_2 molar ratios (0.27 and 0.21, respectively) equal to the ratios in SON68 glass, the inactive reference for the French R7T7 high-level waste containment glass. Glass compositions were obtained by progressively adding Al, Ca, and Zr, with the same concentrations as in SON68 glass. Consequently, glasses contained either three (a ternary sodium borosilicate glass designated T), four (with aluminum added, designated TAl), 5 (with calcium added, designated TAlCa) or six oxides (with zirconium added, designated TAlCaZr). Glasses were prepared from powder mixtures of SiO_2, H_3BO_3, Na_2CO_3, Al_2O_3, CaO, and ZrO_2 melted in a platinum crucible and refined for 3 h. The process temperatures ranged from 1400 to 1500 °C. The samples were annealed for 1 h in graphite crucibles between 530 and 590 °C ($T_{anneal} = T_g + 20$ °C). The glass samples were chemically analyzed by alkaline fusion ($NaOH + KNO_3$ and $Li_2B_4O_7$, $5H_2O$) of glass powder, then recovered in HNO_3 for ICP-AES analysis. The glass compositions are indicated in Table 1.

2.2. Glass alteration

Glasses were ground with tungsten carbide balls then sieved to recover the size fraction less than 20 μm. This size fraction (<20 μm) was washed in acetone to eliminate the finest glass particles and eventually rinsed with absolute ethanol. Two glass powder size fractions were used to obtain gels. One corresponded to the size fraction less than 20 μm and the other one to a size fraction less than 4 μm. The latter was obtained by settling of the size fraction less than 20 μm in acetone using the Stokes' law. The specific surface area of these two glass powder size fractions was

Table 1
Molar composition of glass specimens

Glass	SiO_2 (mol%)	B_2O_3 (mol%)	Na_2O (mol%)	Al_2O_3 (mol%)	CaO (mol%)	ZrO_2 (mol%)
T	67.7	18.0	14.3	—	—	—
TAl	64.9	17.3	13.7	4.1	—	—
TAlCa	61.2	16.3	12.8	3.9	5.8	—
TAlCaZr	60.1	16.0	12.7	3.8	5.7	1.7

Table 2
Alteration gel formation characteristics (a: acidic-leached glasses, b: basic-leached glasses)

Parameter	TAl-a	TAlCa-a	TAlCaZr-a	T-b	TAl-b	TAlCa-b	TAlCaZr-b
Glass mass (g)	2	2	2	9	40	9	40
Alteration solution volume V (L)	1.0	1.0	1.0	1.0	1.0	1.0	1.0
SA/V (cm^{-1})	64	64	77	81	504	81	380
Renewal rate of solution	Static	Static	Static	1/month	3/week	0.5/week	2/week
Alteration rate ($g\ m^{-2}\ d^{-1}$)	0.013	0.0064	0.0087	0.017	0.019	0.0042	0.00074
Alteration time (days)	59	56	56	178	96	334	1401
Alteration (%)	100	65	75	96	93	83	87
$pH^{90°}$ Start–end	1.09–1.26	1.09–1.21	1.09–1.23	9.1–8.4	8.8–8.1	9.1–8.6	8.7–7.6
[Si] Start–end ($mg\ L^{-1}$)	0–178	0–189	0–206	305–110	97–31	113–26	69–17

The SA/V parameter corresponds to the ratio of the glass surface area (SA) to the alteration volume (V). The silicon concentrations (and pH) for the basic-leached glasses were analyzed after the first ([Si] start) and the last ([Si] end) solution renewal.

measured by BET (Brunauer et al., 1938) method, based on adsorption isotherm of nitrogen. Gels were formed in slightly basic media at pH values generally between 8 and 9, and in highly acidic media (pH 1). Glass powder size fraction not exceeding 4 μm were used for acidic-leached glasses, for about two months at 90 °C in static mode (0.1 mol L^{-1} HNO_3 solution). Glass powder size fractions not exceeding 20 μm were used for basic-leached glasses at 90 °C with renewed ultrapure water. Following glass alteration the gels were oven-dried for 24 h at 90 °C. Some gels were heated a second time for 60 h at 180 °C for NMR proton experiments.

The glass alteration conditions are listed in Table 2. Alteration conditions have been defined to provide as much gel as possible to minimize the contribution of the pristine glass and to obtain gels which develop similar alteration rates. These rates had to be sufficiently low compared with the maximal alteration rate for which very little gel would have been obtained, but high enough to obtain gels under reasonable time periods. The experimental conditions (leaching solution renewal rate and the ratio of the glass surface area to the solution volume, SA/V) have thus been fixed to maintain an alteration rate of approximately two orders of magnitude below the maximal alteration rate, except for the basic-leached glass containing zirconium which is much more resistant to the alteration rate (4 years of alteration were needed). Usually, increasing SA/V ratio leads to a more rapid drop in the glass alteration rate whereas increasing the solution renewal rate increases the alteration rate (Delage et al., 1992; Gin, 2000). The quantity of altered glass was calculated from the boron release, as boron is a good glass alteration tracer (Scheetz et al., 1985). Gels were observed by SEM and no secondary phases were detected on their surfaces. Gels were also analyzed by XRD and all patterns were characteristic of amorphous material with the presence of a bump between about 15° and 40° and the absence of diffraction peaks.

2.3. High-resolution solid-state magic-angle spinning NMR experiments

Most of the spectra were acquired on a Bruker Avance 500 (11.75 T) NMR spectrometer, using a 4 mm (diameter of the ZrO_2 rotor) Bruker CPMAS probe at sample rotation frequencies 12.5 kHz. Some ^{27}Al MQMAS spectra were acquired on a Bruker Avance 300 (7.05 T) NMR spectrometer under similar conditions. Acquisition parameters and experiments performed for each nucleus are described below. The nuclear spin (I) and Larmor frequency (ν_0) of each nucleus are indicated in parentheses. The average sample mass was 100 mg.

^1H ($I = 1/2$, 499, 14 MHz) MAS NMR spectra were acquired with an antiringing suppression. This method was found to be efficient for suppressing the probe ^1H background signal. This experiment was carried out using the pulse sequence 90–*FID*–d_1–180–d_2–90–*FID* with a 180° shift of the phase receiver during the acquisition of the second *FID*. The delay d_1 exceeded the spin relaxation time T_1; this corresponds to two independent *FID* measurements, and the delay d_2 is much smaller that T_1 (here 20 ms). Comparing empty spinning rotor spectra with "full rotor" spectra showed that the residual proton signal (probe and empty rotor) was completely negligible in intensity compared with the sample signal. Rotor-synchronized ^1H Hahn echo MAS spectra were also acquired using the Hahn echo (90–τ–180–τ–*FID*) pulse sequence. The latter was also found to be effective in suppressing the probe background but was mainly used to contrast protons according to the strength of their (homonuclear) dipolar interactions with neighboring protons (^1H dipolar dephasing experiment (Bronniman et al., 1988)): the signal of protons experiencing stronger homonuclear interactions decreased faster. Varying the echo delay is extremely useful for distinguishing the different underlying species of an unresolved ^1H MAS NMR spectrum. To this aim, spin locking experiments are also useful: the decay of the magnetization is characterized by the rotating-frame relaxation time, generally denoted $T_1\rho$, which is both sensitive to the mobility of the proton and to the strength of homonuclear dipolar couplings. These experiments were also performed for analysis of the ^{29}Si CPMAS data (see below) to determine the proton species which have sufficiently long $T_1\rho$ times which can be involved in a cross-polarization transfer. DQ NMR correlation experiments were also performed using the *BABA* pulse sequence (Feike et al., 1996) and were found very useful to identify the proton

species interacting with each other. The principle of DQ spectroscopy is to correlate the spectrum of pairs of protons to the spectrum of the individual protons involved in the pairs. Rotor-synchronized acquisition in the first dimension was used, yielding a spectral width of 12.5 kHz which was found to be sufficient considering the MAS spectra width of less than 6 kHz (12 ppm). Typically, 64 t_1 *FIDs* were acquired. For all experiments, the length of the radiofrequency (*rf*) pulses was chosen to be 4.5 μs for 90° pulses (*rf* field strength of 55 kHz). Typically, 64–256 *FIDs* were acquired in 2D experiments for each t_1-slice and 32–1024 *FIDs* in 1D experiments. Recycle delays of 1 s (2 s) were found to allow complete relaxation of the protons in undried samples (heated samples, respectively). Proton chemical shifts were referenced using an external sample of tetrakis(trimethylsilyl)silane (0.2 ppm relative to liquid tetramethylsilane, TMS).

^{29}Si ($I = 1/2$, 99.165 MHz) MAS NMR measurements were performed on all samples using an antiringing pulse sequence (see the previous section for a short description, with $d_2 = 20$ ms) using a recycle delay of 20 s. This delay was not sufficient to allow complete relaxation but longer recycle delays were found to yield identical spectrum shape. Cross-polarization (from proton) spectra were also collected with varying contact time, typically 2 and 8 ms to discriminate silicon species according to their proximity to protons. Typically, 2048 *FIDs* were acquired. The *rf* pulse length was 5 μs for 90° pulses. During cross-polarization, the *rf* fields were 37.5 and 25 kHz for ^{1}H and ^{29}Si, respectively. The mismatch of the *rf* field equal to the spinning frequency was found to ensure the most efficient transfer between the two nuclei under fast MAS. A 5 kHz ^{1}H decoupling field was also found to be sufficient during acquisition. HETCOR spectra were recorded, with a contact time of 8 ms, to determine the proton species involved in the magnetization transfer of each silicon species. Rotor-synchronized acquisition in the first dimension was used (spectral width 12.5 kHz), 1024 *FIDs* were accumulated for each of the 32 t_1 slices. Silicon chemical shifts were referenced using an external sample of tetrakis(trimethylsilyl)silane (two peaks at −9.9 and −135 ppm relative to liquid TMS).

^{27}Al ($I = 5/2$, 130.06 MHz at 11.7 T and 78.62 MHz at 7.05 T) MAS NMR spectra were acquired using a short pulse length (0.5 μs) to obtain a quantitative spectra and with recycle delays ranging from 0.5 to 2 s. This was found to be long enough to prevent saturation of the spin system. MQMAS experiments were performed using the Z-filter sequence (p_1–t_1–p_2–τ–p_3) (Frydman and Harwood, 1995; Amoureux et al., 1996). The first and the second excitation pulse were experimentally adjusted to $p_1 = 4.5$ μs and $p_2 = 1.6$ μs (*rf* field strength of 75 kHz), followed by one rotor period (τ) Z-filter delay, and a third soft pulse $p_3 = 5.5$ μs (*rf* field strength of 15 kHz). The spectral width of the first dimension was set to 100 kHz, 256–512 *FIDs* were accumulated for each of the 160 t_1-slice. Reference convention of (Massiot et al. (1996)) was used in the first dimension. For ^{1}H–^{27}Al cross-polarization experiments, *rf* field strengths and contact time were experimentally optimized, 14.5 kHz (^{1}H), 2 kHz (^{27}Al) and a contact time of 800 μs. Aqueous $Al(NO_3)_3$ 1 M was used as external reference for ^{27}Al NMR spectra.

3. Results and discussion

3.1. Leaching experiments

The quantity of altered glass was calculated from the boron released into solution and is plotted versus time in Fig. 1. The boron normalized mass loss $NL(\mathrm{B})$ (in g m^{-2}) is given by:

$$NL(\mathrm{B})(g/m^2) = \frac{[B]}{\tau(B) \times \frac{SA}{V}},$$

where $\tau(\mathrm{B})$ is the fraction of boron in the pristine glass, [B] is the boron concentration in the solution (g m^{-3}) and SA/V the ratio of the glass surface area to the solution volume (m^{-1}). The quantity of altered glass (QAG) is calculated from the proportion of boron released. Considering the glass grains as spheres, the variation of their radius versus time is estimated using a shrinking core model from which the evolution of the surface area of pristine glass can be calculated. The gel chemical composition was calculated from the element concentrations as determined by ICP-AES in the leachates. The quantity of an element remaining in the gel is considered equal to the difference between its concentration in glass and in solution. The amount M_{gel} (i) (in

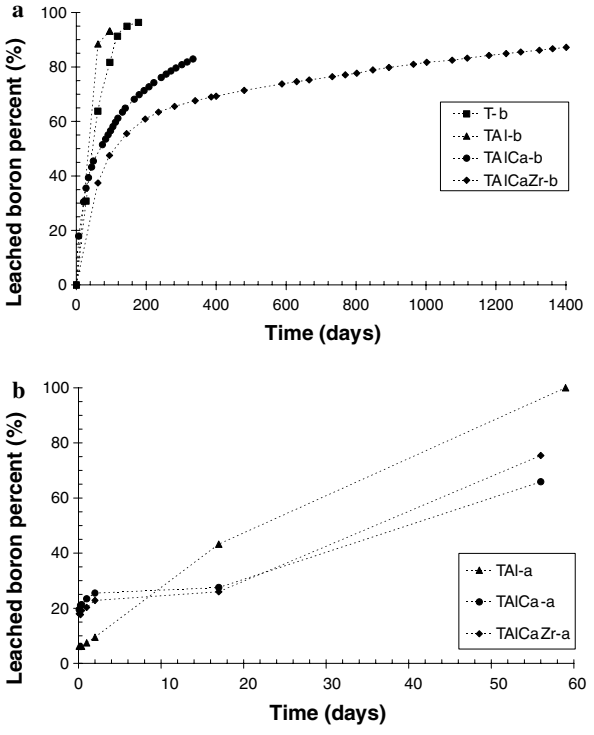

Fig. 1. Quantity of altered glass from the boron released into solution for basic (a) and acidic (b) leached glasses.

Table 3
Molar composition (oxides and elements) of alteration gels, determined from elements analyzed in solution (a: acidic-leached glasses, b: basic-leached glasses)

Gel	SiO_2 (mol%)	B_2O_3 (mol%)	Na_2O (mol%)	Al_2O_3 (mol%)	CaO (mol%)	ZrO_2 (mol%)
TAl-a	100.0	0.0	0.0	0.0	—	—
TAlCa-a	100.0	0.0	0.0	0.0	0.0	—
TAlCaZr-a	93.0	0.0	0.0	0.0	0.0	7.0
T-b	100.0	0.0	0.0	—	—	—
TAl-b	87.7	0.0	6.1	6.2	—	—
TAlCa-b	85.7	0.0	0.8	5.7	7.8	—
TAlCaZr-b	72.9	0.0	0.7	6.5	13.8	6.1

grams) of a gel constituent element i can be calculated from the solution concentrations and n solution renewals according to the following relation:

$$M_{\mathrm{gel}}(\mathrm{i}) = \left(1 - \frac{\sum_{j=1}^{n} V_j \times [\mathrm{i}]_j \Big/ M_{\mathrm{glass}}(\mathrm{i})}{\sum_{j=1}^{n} V_j \times [\mathrm{B}]_j \Big/ M_{\mathrm{glass}}(\mathrm{B})}\right) \times M_{\mathrm{glass}}(\mathrm{i}),$$

where V_j is the solution volume of the jth renewal, $[\mathrm{B}]_j$ and $[\mathrm{i}]_j$ (g L^{-1}) correspond to the concentration of boron and element i in the jth sampling, $M_{\mathrm{glass}}(\mathrm{B})$ and $M_{\mathrm{glass}}(\mathrm{i})$ (g) represent the mass of boron and element i in the glass.

T and TAl glasses were leached at a similar rate at basic pH (designated T-b and TAl-b). Adding calcium (TAlCa-b) caused the glass alteration rate to drop by a factor of about five compared with TAl-b; the further addition of zirconium (TAlCaZr-b) resulted in an additional drop by a factor of 5 in the alteration rate compared with TAlCa-b or a factor of 25 compared with T-b. The alteration rates of TAl, TAlCa, and TAlCaZr glasses at acidic pH (designated TAl-a, TAlCa-a, and TAlCaZr-a) varied only slightly (between 0.006 and 0.013 g m^{-2} d^{-1}). The quantity of altered glass was linear over time indicating that the gel layer formation did not influence the dissolution rate. Conversely, the evolution of the altered glass in a basic medium shows rather an affinity reaction control and/or silicon diffusion in the gel. The gel chemical compositions are indicated in Table 3. The gels formed in acidic media contained only silicon and zirconium (when the latter was present in the pristine glass); boron, sodium, and aluminum were entirely released into solution. Gels obtained in basic media, TAlCa-b and TAlCaZr-b, contained eight times fewer sodium atoms than aluminum atoms, whereas TAl-b contained equal amounts of both. In addition, TAlCa-b and TAlCaZr-b contained, respectively, 5 and 10 times more calcium than sodium. Regardless of the alteration conditions, silicon is the major element in the gels.

3.2. Solid-state nuclear magnetic resonance spectroscopy

3.2.1. ^1H MAS NMR

Fig. 2 displays ^{1}H MAS NMR spectra acquired with different methods: direct acquisition (DA) obtained with the antiringing sequence (Fig. 2a), rotor-synchronized Hahn echo (HE) (Fig. 2b), and spin locking sequence (SL) (Fig. 2c). Whereas DA spectra of basic and acidic-leached samples are similar, it is evident that HE and SL data are very useful for discriminating several groups of resonances (exhibiting very different behaviors) underlying the DA spectra, and they more clearly reveal differences between the basic and acidic-leached samples. Other HE and SL data were collected with varying spin echo and spin locking delays to investigate the behavior of each resonances. Only the most representative are displayed here. The width of

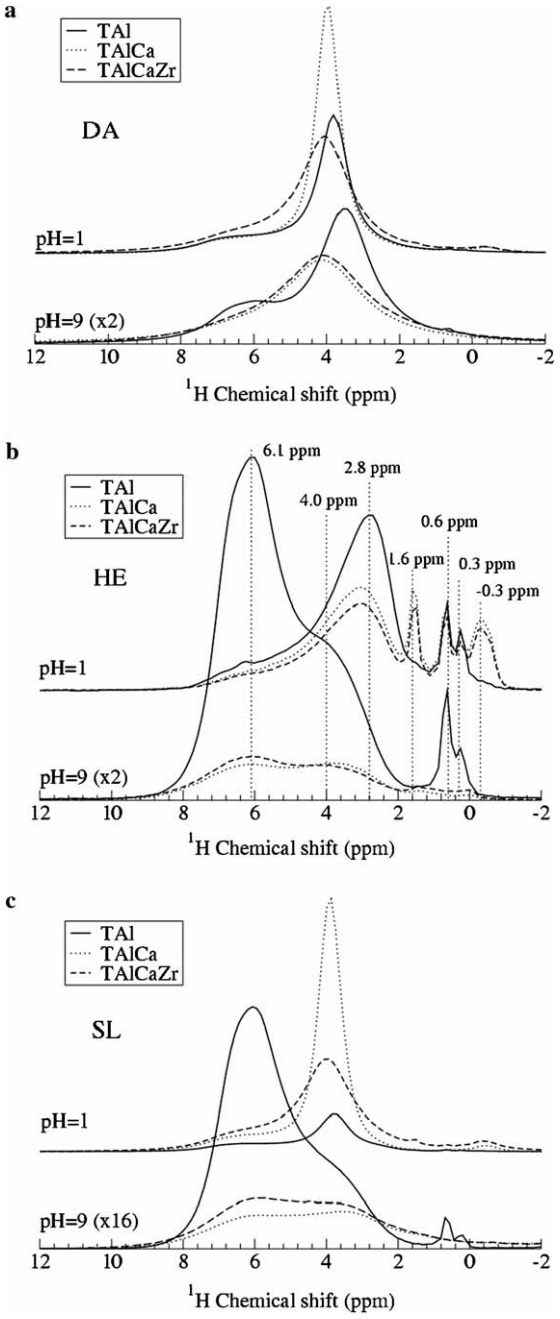

Fig. 2. ^{1}H MAS spectra of acidic and basic-leached glasses acquired with a direct acquisition (DA) using the antiringing sequence (a), rotor-synchronized Hahn echo (HE) sequence with an echo delay of 4 ms (b) and after a spin locking (SL) period of 8 ms (c). All spectra are normalized to the same sample mass.

these lines results mainly from chemical shift dispersion and reflects the broad distribution of the proton environment.

3.2.1.1. Basic-leached glasses. In basic-leached glasses, four groups of resonances can be resolved (Fig. 2b). Two narrow peaks at about 0.3 and 0.6 ppm are observed for TAl-b, whereas a very low-intensity broad resonance between 0 and 1.4 ppm is observed for TAlCa-b and TAlCaZr-b. It should be pointed out that the area of these peaks is less than 0.5% in the DA spectra (it has been checked that these peaks does not correspond to the fingerprints and the rotors were cleaned before use), and are therefore indicative of proton species with a very small population, and not accessible to molecular water. Taking into account the long transverse relaxation time of these peaks, they can be attributed to non-hydrogen bonded silanols groups, also called *isolated* silanols or free hydroxyl groups. The other two peaks are broad with maximum height at about 6–6.5 and 3.5–4.5 ppm. The faster decay of the later peak in HE and SL data is indicative of stronger ^{1}H–^{1}H dipolar couplings and it can thus be attributed to molecular water bound to the pore surface by hydrogen bonds. A similar peak at 4.2 ppm was observed in hydrated silica (Kohn et al., 1989a) and assigned to molecular water bound to the silicate network by hydrogen bonds. Similarly, such a peak has also been attributed to molecular water on the surface of fine particles of silica (*Cab-O-Sil* fumed silica) (Liu and Maciel, 1996) or silica gel (Bronniman et al., 1988), on hydrated soda glasses (Schaller and Sebald, 1995; Robert et al., 2001) and on hydrated albite glasses (Zeng et al., 1999). This peak is relatively broad and its symmetrical lineshape suggests that homonuclear dipolar couplings are mainly responsible for its width. Furthermore, the absence of a narrow peak at about 5 ppm shows that all the free water was removed when samples were dried at 90 °C. The difference in position of this peak between TAl-b (~3.5 ppm) and TAlCa-b, TAlCaZr-b (~4 ppm) (Fig. 2a) may be related to the difference of composition in cation species. TAl-b contained only sodium cations whereas TAlCa-b and TAlCaZr-b contained only calcium cations. A similar difference is also observed in the water peak width, suggesting stronger dipolar couplings. The second peak at 6–6.5 ppm can be assigned to silanol sites where the proton is hydrogen bonded to another oxygen. Such resonances were observed by Zeng et al. (1999) in aluminosilicate glasses.

Double quantum experiments were performed to probe the spatial proximities between the proton species and to gain insight into the hydrogen bonding interactions (Fig. 3). In these experiments, the spectrum of pairs of dipolar coupled protons (yielding the double quantum dimension) is correlated to the spectrum of the individual proton (single quantum or MAS dimension) involved in each observed pair. The chemical shift of a DQ resonance in the first dimension is simply the sum of the two chemical shifts of the two individual protons. The intensity of a DQ

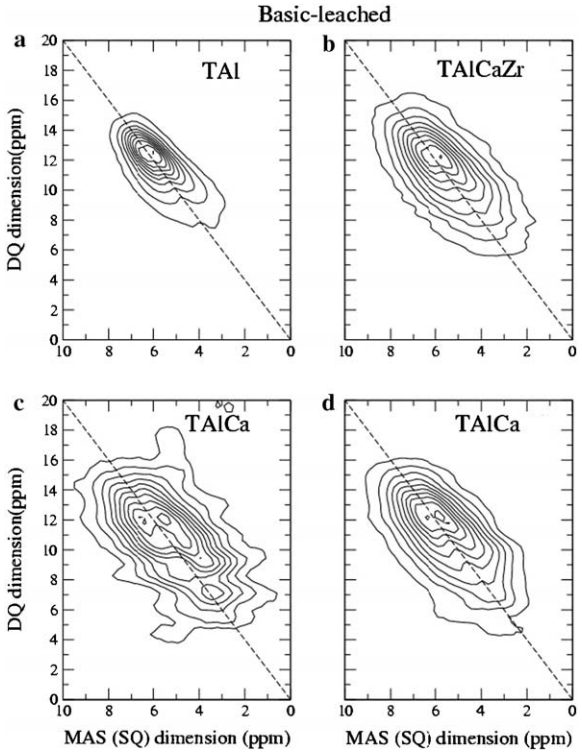

Fig. 3. ^{1}H double-quantum (DQ) MAS spectra of basic-leached glasses. TAl (a), TAlCa (d), and TalCaZr (b) have been acquired using a double quantum excitation period of two rotor periods (160 μs), and of one rotor periods for TAlCa (80 μs) (c). Equally spaced contour levels are drawn from 9.8% to 98% of the maximum height. The chemical shift of a DQ resonance is the sum of the two chemical shifts of the two individual protons. DQ resonance of pairs of two sites belonging to the same species are on the dashed line (the autocorrelation line).

resonance depends mainly on the strength of the dipolar coupling between the two nuclei involved and on the duration of the excitation period of the DQ resonances. To some extent, the latter has to match the desired range of dipolar couplings. This is illustrated by Figs. 3c and d for TAlCa-b. DQ spectrum Fig. 3c was acquired using a shorter preparation period (80 μs instead of 160 μs). In (Fig. 3c), the molecular water peak involving the two water protons is of higher intensity (reflecting the fact that the dipolar coupling between these two protons is higher than the one involved in other pairs). We chose a preparation period that gives rise to the highest DQ signal intensity, which was found to be the same for all basic-leached samples. This reveals that dipolar coupling are of the same order of magnitude in all samples. In all DQ spectra, the highest intensity plot is around 6–6.5 ppm, reflecting the existence of dipolar interactions between silanol protons. As a result of both the interaction of silanol groups with protons of molecular water and the distributed chemical shift of protons, DQ spectra are aligned along the autocorrelation line (dashed line) with a width that depends upon the distribution of the chemical shift of the two species involved. For TAl-b, narrower spectra is observed as a consequence of the much lower intensity of the molecular physisorbed water peak.

3.2.1.2. Acidic-leached glasses. Spectra of acidic-leached glasses exhibit the same group of resonances, but additional peaks are revealed by the HE spectra (Fig. 2b). Narrow peaks are observed at about 0.3 and 0.6 ppm, but also at 1.6 and −0.3 ppm for TAlCa-a and TAlCaZr-a. As for basic-leached samples, each of these peaks is representative of no more than 1% of the protons detected in DA spectra (Fig. 2a), and represent proton sites that are not accessible to molecular water. The fact that these peaks decrease significantly in the SL spectra (Fig. 2c) suggests that they are characterized by higher mobility than other species (leading to a shorter $T_1\rho$ time (Klur et al., 2000) but to a slower decrease in HE experiments as a result of the motional averaging of the dipolar couplings). The two broad peaks observed at about 4 and 6.5 ppm can be assigned accordingly to basic-leached samples. One should note the difference in the linewidth of the molecular water lines between the samples (Figs. 2a and c). Such a difference can be related to the specific area measurements (Table 4) suggesting that TAlCaZr-a has lower pore sizes than TAl-a and TAlCa-a (which exhibit a similar linewidth for molecular water). Usually, when zirconium is present in the gel, the specific surface area is greater and the pores smaller, of a few nanometers (Spalla et al., 2004). Moreover, the fact that the TAl-a peaks is of much lower intensity than TAlCa-a and TAlCaZr-a in Fig. 2c results from a shorter $T_1\rho$. This means that water mobility is higher in this gel, as a consequence of a higher mean pore size. As to basic-leached glasses, a rapid decrease of the molecular water peak is observed in HE data. However, such a fast decrease is also observed for the silanol peaks, implying stronger dipolar couplings. This is also observed in the DQ data displayed in Figs. 4a and b dominated by a strong correlation of the water peak with the silanols peak. The fact that the proton chemical shifts of silanol groups in acidic-leached glasses, ranging from 4 to 8 ppm, is the same as observed in basic-leached glasses implies that strengths of hydrogen bonds are of same order magnitude in both series. Strengthening of the dipolar coupling can thus be explained by a decrease of the mobility of the proton species (silanol and molecular water) is acidic-leached glasses leading to a long $T_1\rho$ but a rapid decay of the echo. HE spectra shown in Fig. 2b are dominated by a broad asymmetrical peak with maximum height at 2.8–3 ppm. This peak is characterized by a slow decrease, longer than silanol group in basic-leached samples. The proton spectrum of hydrated silica containing 1200 ppm of water only in the form of Si–OH (Suprasil) exhibits a narrow peak at 3.3 ppm (Kohn et al., 1989a). In SiO_2 glass containing 2.5 wt% water, the Si–OH contribution appears at 3.1 ppm (Kohn et al., 1989a). Since the composition of these gels is the same as the hydrated silica (except for TAlCaZr-a, which also contains zirconium), this peak can be attributed to Si–OH species. No displacement of the ^{1}H resonance toward increasing chemical shifts, corresponding to strong bonds such as hydrogen bonds between Si–OH and a non-bridging oxygen (Ai et al., 2004), was observed in any of the altered glass samples in this study. The number of non-bridging oxygens is probably very small because of the rapid formation of hydroxyl groups.

Table 4
Specific surface area of acidic-leached glasses (BET measurements)

Gel	TAl-a	TAlCa-a	TAlCaZr-a
Specific surface area (m^2/g)	155 ± 8	278 ± 14	339 ± 17

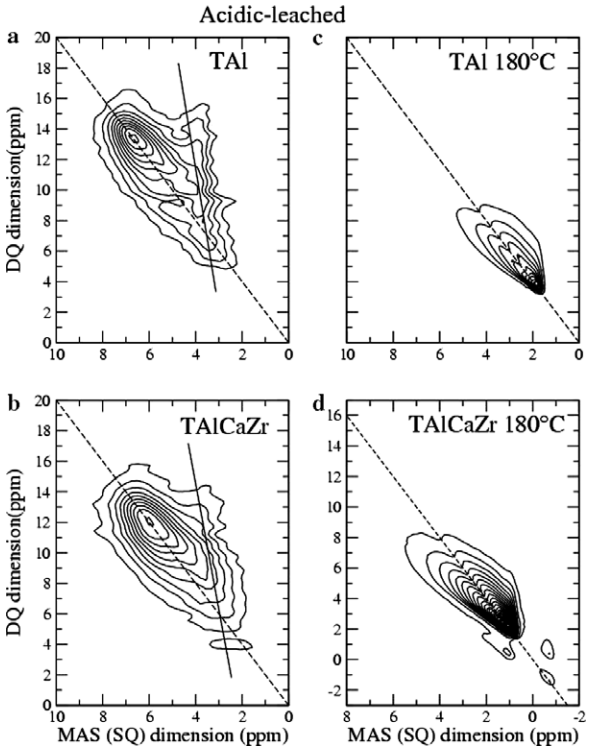

Fig. 4. ^{1}H double-quantum (DQ) MAS spectra of acidic-leached glasses TAl (a) and TAlCaZr (b), and of heated (180 °C) TAl (c) and TAlCaZr (d). All spectra have been acquired using a double quantum excitation period of two rotor periods (160 μs). Equally spaced contour levels are drawn from 9.8% to 98% of the maximum height. The chemical shift of a DQ resonance is the sum of the two chemical shifts of the two individual protons. Dashed line is the autocorrelation line and solid line highlights the interaction (hydrogen bond) between water molecules and silanol groups.

In order to assess our assignments, the gels were heated for 60 h at 180 °C to evaporate the physisorbed molecular water. Fig. 5 shows the ^{1}H spectra for TAl and TAlCaZr gels. Two main peaks are observed: a broad asymmetrical peak with maximum height at 2.8–3 ppm, and a narrow peak at 1.6–1.8 ppm. A weak broad peak at 6 ppm can still be seen. The strong attenuation of this peak and disappearance of the molecular water peak at 4 ppm is consistent with the rupture of the hydrogen bonds between silanol groups and water molecules. This confirms the attribution of the 6 ppm peaks to hydrogen-bonded hydroxyl groups. From the seminal work of Maciel et al. (Chuang et al., 1993; Liu and Maciel, 1996; Chuang and Maciel, 1997), the narrow peak at 1.6–1.8 ppm is assigned to free hydroxyl groups (non-hydrogen bonded) and 2.8 ppm to silanols

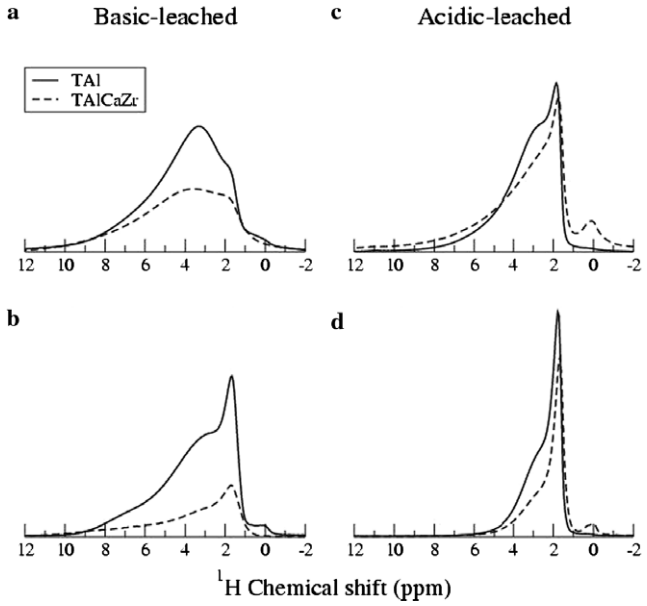

Fig. 5. ^{1}H MAS spectra of basic (left) and acidic (right) leached TAl and TAlCaZr glasses heated for 60 h at 180 °C, acquired using the antiringing sequence (a and c) and rotor synchronized Hahn echo sequence with an echo delay (or refocusing time) of 4 ms (b and d). All spectra are normalized to the same sample mass.

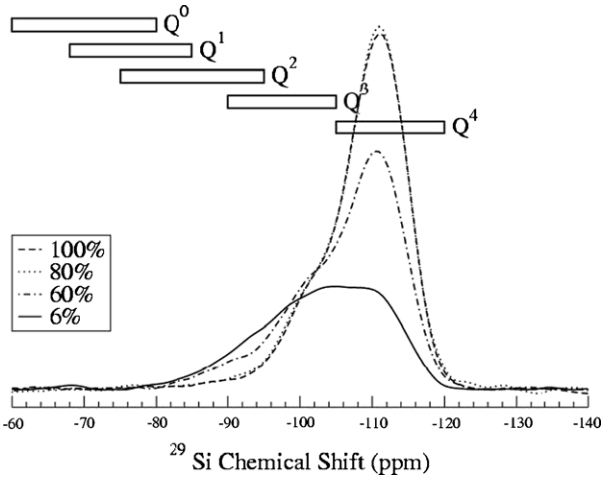

Fig. 6. ^{29}Si MAS spectra of ternary glass during alteration at basic pH (T-b). The percentage of altered glass is indicated in the key. The spectra have been normalized to the same sample mass.

weakly hydrogen bonded to one another. These interactions are shown on DQ spectra in Figs. 4c and d for acidic-leached glasses (similar data were obtained for basic-leached glasses). It is worth noting that a small resonance near 0 ppm is observed for TAlCaZr-a only, and a correlation of this peak with the free hydroxyl peak is clearly observed in DQ spectrum (Fig. 4d). This site could be related to zirconium.

3.2.2. ^{29}Si MAS NMR

The chemical shift of ^{29}Si is affected by the silicon coordination number, by its first neighbors (bridging and non-bridging oxygen) and by the nature of the second neighbors (with other formers such as aluminum inserted in the silicate network). The Q^n species (where $n = 0$–4 is the number of bridging oxygens) all exhibit different chemical shifts, and can thus theoretically be separated by NMR. Separating the chemical shifts of different sites is not difficult in binary glasses, which exhibit a clear shift from Q^4 species to Q^1 species when alkalis are added (Maekawa et al., 1991). In systems containing more oxides it becomes increasingly difficult to discriminate between the contributions of each site. Their distributions are superimposed and the resolution is therefore significantly reduced. The problem is even more complex in compounds containing other types of formers inserted in the silicate network. Because of their different electronegativity, the chemical shift of silicon diminishes. This effect is particularly well known for aluminum (Engelhardt and Michel, 1987). Overlapping can occur, for example, between Q^3 with Si as second neighbor and Q^4 with Al as second neighbor. It is not annoying here because the quantity of Al is low in comparison with Si and, more importantly, the Al/Si ratio is closed in our samples. Fig. 6 shows the evolution of the ^{29}Si MAS spectra of the ternary glass during alteration at basic pH (T-b). The spectra in direct acquisition probed the entire sample; the resulting signal represents the contribution from the pristine and the leached glass, except in the 100% altered glass. The progression toward increasingly polymerized species in the alteration gel is clearly visible. A comparable progression is also visible on other gels leached in basic or acidic conditions as shown in Fig. 7f for TAl (similar spectra were obtained for TAlCa and TAlCaZr). The spectra have been normalized to the same sample mass; the increasing peak area thus indicates silicon enrichment in the gel.

3.2.2.1. Pristine glasses. The comparison of pristine glasses (Fig. 7c) shows that there is a shift toward increasing chemical shifts for TAlCa with regard to TAl glass, reflecting a lesser degree of polymerization of the TAlCa network. This can be attributed to the addition of calcium, which increases the total quantity of network modifiers available to depolymerize the network. The spectrum of TAlCaZr is very close to that of the TAlCa glass, although an increase (in average) of the chemical shift can be expected from the increased polymerization: zirconium mobilizes cations—which are no longer available as network modifiers—for charge compensation of the $[ZrO_6]^{2-}$ octahedra sharing corners with SiO_4 tetrahedra (Galoisy et al., 1999). Zr as a second neighbors thus shifts the silicon peaks toward higher chemical shifts as does aluminum (Engelhardt and Michel, 1987).

3.2.2.2. Acidic-leached glasses. For all types of acidic-leached glasses and virtually irrespective of the initial glass composition, all gel spectra exhibit well resolved Q^2, Q^3, and Q^4 peaks allowing unambiguous quantification. The non-bridging oxygen of these $Q^{(n)}$ species have probably

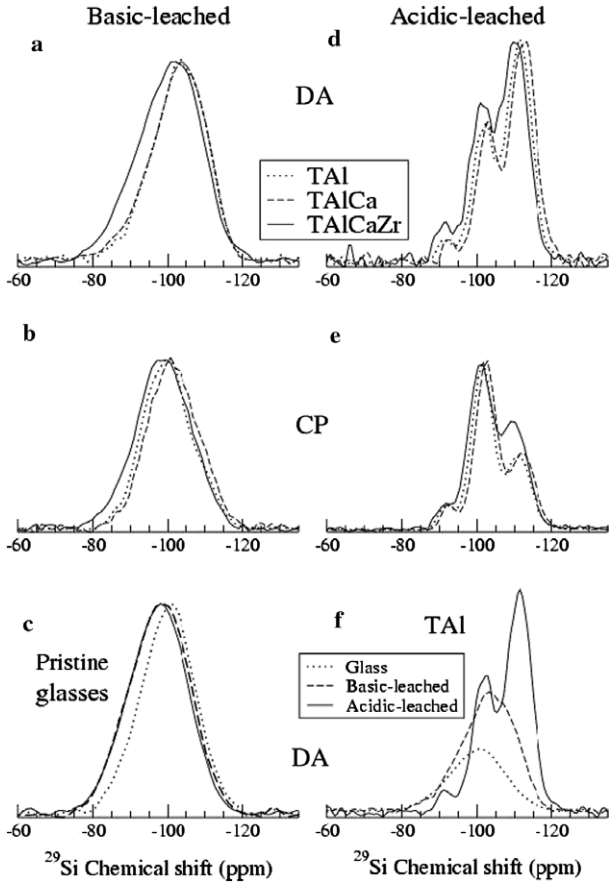

Fig. 7. ^{29}Si MAS spectra of pristine (c), basic (a) and acidic-leached (d) TAl, TAlCa and TAlCaZr glasses. (f) Compares TAl glass with TAl gels (direct acquisition, DA). ^{29}Si CPMAS spectra obtained with proton-to-silicon magnetization transfer times of 8 ms are given for basic (b) and acidic-leached (e) glasses (CP). The spectra have been normalized to the same sample mass.

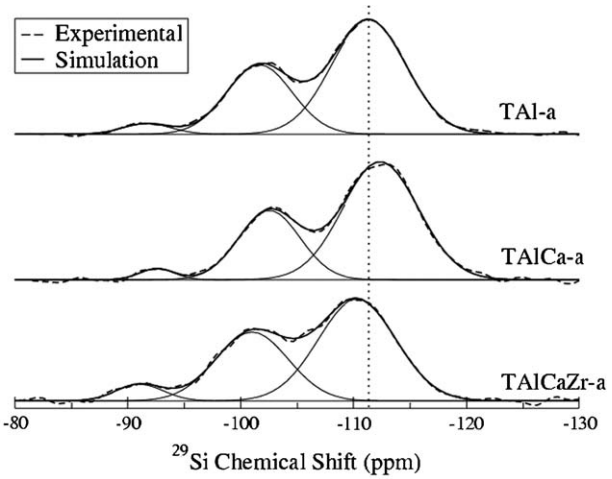

Fig. 8. Experiment and simulated ^{29}Si MAS spectra of acidic-leached glasses. Each line has been fitted to a gaussian lineshape with parameters given in Table 5.

Table 5
Quantification of Q^n species in the acidic-leached glasses by simulation of ^{29}Si MAS spectra (from Fig. 8)

	TAl-a	TAlCa-a	TAlCaZr-a
Q^2 proportion (%)	3.7	2.8	5.8
Line position (ppm)	−91.7	−92.6	−91.1
Peak width (ppm)	2.1	1.5	2.1
Q^3 proportion (%)	33.2	31.1	36.3
Line position (ppm)	−101.6	−102.5	−101.0
Peak width (ppm)	2.9	2.7	3.2
Q^4 proportion (%)	63.0	66.1	58.0
Line position (ppm)	−111.3	−112.4	−110.3
Peak width (ppm)	3.3	3.4	3.4

reacted with protons to form OH groups. We conserve here the same designation for $Q^{(n)}$: for example, Q^3 species in gels are composed of three siloxane bonds and one hydroxyl bond. NMR measurements of other nuclei did not detect the presence of aluminum, boron, and sodium in these gels. Fig. 8 shows the experimental and simulated spectra used for quantification of the acidic-leached glasses (Table 5). The proportion of each species is of the same order of magnitude for all the alteration gels. Nevertheless, some differences can be noticed. Although only TAl-a is 100% leached, TAlCa-a (65% leached) is richer in Q^4 species whereas TAl glass is more polymerized than TAlCa glass. It seems that during acidic leaching, the most depolymerized glass produced the most polymerized gel. The higher initial proportion of network modifiers thus appears to favor silicon repolymerization. Our results are in agreement with the mechanism proposed by Bunker et al. (1988) for sodium borosilicate glass leached in acidic media. The authors suggested that the repolymerization increases with the number of silanols created during leaching. Glasses with higher modifier content (resulting in a higher silanol content) should thus be more susceptible to repolymerization. As previously observed for pristine glass, a shift toward higher chemical shift is observed in Fig. 8 for TAlCaZr-a gel. In addition, the larger proportion of Q^3 species in TAlCaZr-a can be explained by a rupture of some of Si–O–Zr bonds after zirconium release, possibly leading to ZrO_2 precipitation as observed on R7T7 glass leached at high solution renewal rates (Pelegrin, 2000). However, the influence of zirconium on the ^{29}Si chemical shift suggests that a part of the Zr inserted in the silicate network forms Zr–O–Si bonds. Accordingly, a fraction of the zirconium would participate to the network formation along with silicon while some zirconium would be hydrolyzed. However, our experiments cannot discriminate between these two mechanisms (Zr-Si copolymerization or ZrO_2 precipitates).

^{1}H–^{29}Si Cross-polarization (CP) spectra were recorded to elucidate the silicon environment according to proton proximities. As shown in Fig. 7e, Q^3 and Q^2 are polarized more efficiently than Q^4 species because of their stronger (hetero-)dipolar coupling with neighboring protons. TAlCaZr-a has a larger number of protons near Q^4 sites than TAl-a and TAlCa-a. TAlCaZr-a is more porous (higher specific surface), and ''bulk gel'' may therefore be

more accessible to the surface proton species. Varying the contact time is a widely used technique to gain more insight into the different proton species involved in the magnetization transfer process (see for example Cody et al., 2005). However, such information can be obtained as well with ^{1}H–^{29}Si CP HETCOR spectroscopy as shown in Fig. 9. The HETCOR map correlates the resonances of the proton species participating to the polarization of each silicon species. The data shown in Figs. 9a and b indicate that both the hydrogen-bonded (HB) hydroxyls (~6 ppm) and HB molecular water (~4 ppm) contribute to the polarization of the silicon Q^2, Q^3 and Q^4 species in all acidic-leached samples (TAlCa-a data not shown). The relative intensities of each line cannot be directly related to information such as distances or quantities, a precise analysis of the CP dynamics is necessary. In fact, a detailed analysis would require the acquisition of several HETCOR maps with different ^{1}H–^{29}Si contact times. It is worth noting that the proton peaks at −0.5 ppm contributes to the polarization of Q^3 and Q^4, but more efficiently to the latter (also observed in Fig. 7e). This HETCOR maps also show the gel with higher specific surface area (TAlCaZr-a) allows a larger proportion of molecular water and especially hydroxyl groups to be near the Q^4 species. After heating at 180 °C, the spectra of both gels were very similar (Figs. 9c and d); all the correlations moved toward the lowest chemical shifts. The protons of the Si–OH groups, whose chemical shift was modified after the release of the physisorbed water molecules, transferred their magnetization to the Q^2, Q^3, and Q^4 sites. The narrow peak at 1.6 ppm is present but only contributes to the polarization of the Q^3 and Q^2 sites. Following the elimination of the water, only silanol groups bound by hydrogen bonds to Si–O–Si or from neighboring Si–OH sites should remain along the Q^4 dimension.

3.2.2.3. Basic-leached glasses. ^{29}Si MAS and ^{1}H–^{29}Si CPMAS spectra of basic-leached glasses are shown in Figs. 7a and b. In contrast to acidic-leached glasses, these gels contain other elements (Al,Ca,Na). The aluminum results in a silicon chemical shift dispersion that makes the discrimination among the $Q^{(n)}$ species much more difficult. Despite the difference in the charge-compensating cation, TAl-b and TAlCa-b spectra are very close, indicating very similar polymerization. TAlCaZr-b exhibits the same shift toward higher chemical shift as observed in glasses (Fig. 7c). The CPMAS spectra are shifted to higher chemical shift as expected from the higher (cross-) polarization of the Q^2 and Q^3 species. However, compared with the TAl-b spectrum, the TAlCa-b spectrum is shifted to lower chemical shift, whereas TalCaZr-b is shifted to higher chemical shift. In fact, for the latter it is difficult to distinguish polymerization change from the effect of zirconium on silicon chemical shift. We favor this second hypothesis in the light of previous results. HETCOR spectra of basic-leached glasses are shown in Fig. 10, along with the

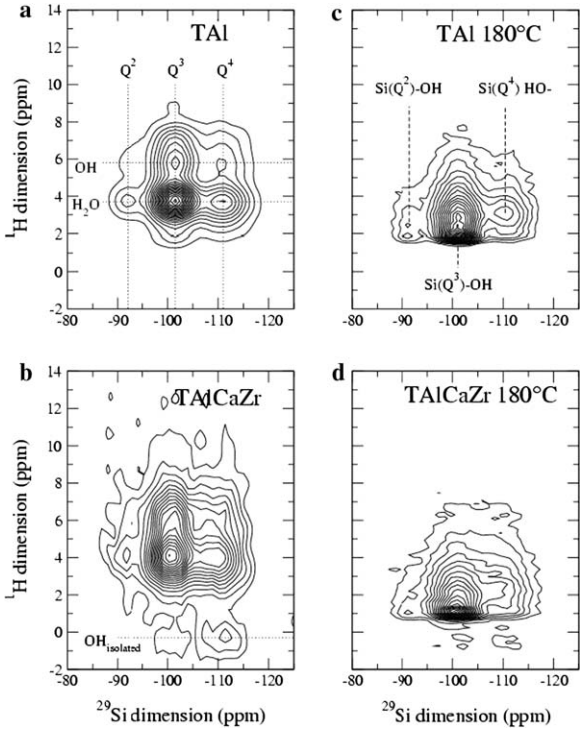

Fig. 9. $^{1}H \rightarrow {}^{29}Si$ HETCOR spectra with 8 ms polarization time for acidic-leached glasses: TAl-a and TAlCaZr-a. (a) TAl-a, (b) TAlCaZr-a, (c) TAl-a heated for 60 h at 180 °C, (d) TAlCaZr-a heated for 60 h at 180 °C. Equally spaced contour levels are drawn from 5% to 100% of the maximum height.

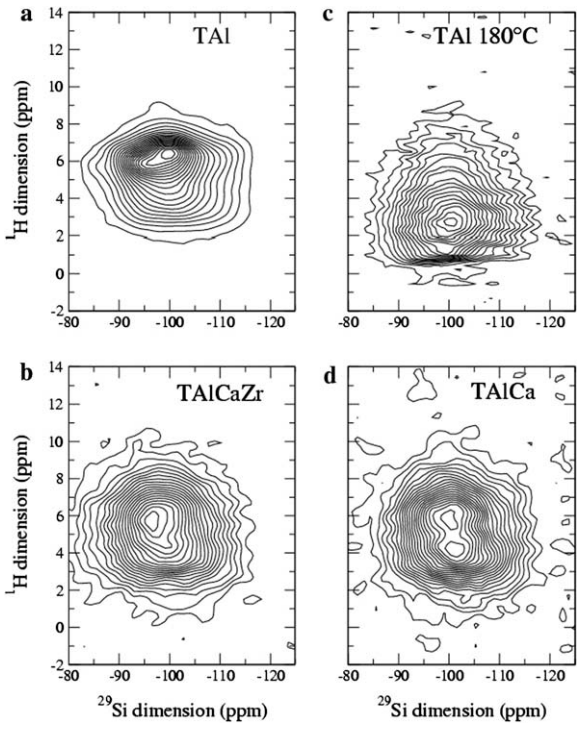

Fig. 10. $^{1}H \rightarrow {}^{29}Si$ HETCOR spectra with 8 ms polarization time for basic-leached glasses. (a) TAl-b, (b) TAlCaZr-b, (c) TAl-b heated for 60 h at 180 °C, (d) TAlCa-b. Equally spaced contour levels are drawn from 5% to 100% of the maximum height.

spectra of heated TAl-b (a similar effect is observed for TAlCaZr-b). Polarization is transferred to silicon atoms from both HB hydroxyl groups (~6 ppm) and HB molecular water (~4 ppm). For heated samples, the same transformation as described for acidic-leached glass is observed.

3.2.3. ^{27}Al MAS NMR

Fig. 11 shows the ^{27}Al MAS spectra of the pristine and basic-leached glasses. The peak positions around 55 ppm correspond to the signature of tetrahedral aluminum (Muller et al., 1981; Engelhardt and Michel, 1987; Oestrike et al., 1987). No peaks were detected around 0 ppm corresponding to aluminum at coordination number 6 (Kinsey et al., 1985; Tsomaia et al., 2003). A small proportion of octahedral aluminum was observed in the alteration gels on the French SON68 inactive nuclear glass doped with Eu^{3+} (Ollier et al., 2003). Nevertheless, octahedral aluminum can also result from the formation of secondary alteration products precipitated on the gel, as is often the case with these complex glasses. No signal was detected for aluminum in acidic-leached glasses; this is consistent with the solution analysis, which indicated that all the aluminum had been leached, as it is commonly observed in acidic media (Hamilton and Pantano, 1997; Abraitis et al., 2000; Hamilton et al., 2001). Fig. 11 clearly shows that the spectra of an alteration gel is narrower than its corresponding pristine glass. This phenomenon is even more pronounced for TAl-b. Conversely, the chemical shift remains relatively close for all the types of glass (altered or not). The differences observed between the spectra cannot be attributed to variations in either the quantity of altered glass or the proportion of aluminum in the glass or gel, since these quantities are very similar for all three compositions. Such a narrowing effect has already been observed in hydrated aluminosilicate glass compositions (Kohn et al., 1989b, Oglesby et al., 2002). Acquiring spectra with two different magnetic fields (taking advantage of the fact that the second order quadrupolar interaction effect is inversely proportional to square of the magnetic field, whereas the chemical shift interaction is directly proportional) showed that this effect could be related to a decrease in either the chemical shift or the quadrupolar interaction (Kohn et al., 1989a,b, 1992; Schmidt et al., 2001; Robert et al., 2001; Oglesby et al., 2002; Padro et al., 2003). Nevertheless, when the physisorbed water was eliminated from the sample by heating at 180 °C, a broadening of the spectrum was observed. The reduction in the ^{27}Al peaks during leaching is thus not a structural effect but is due to the presence of neighboring water. While the spectrum of heated TAl-b was nearly identical with the pristine glass, those of heated TAlCa-b and TAlCaZr-b were broader. As indicated in Table 3, the number of sodium atoms remaining in TAl-b is very close to the number of aluminum atoms. One explanation for this could be that only the sodium compensating the charge of the $[AlO_4]^-$ groups remains in the alteration gel. These cations are known to be less reactive with water than when combined with a non-bridging oxygen (Smets and Lommen, 1982). Concerning TAlCa-b, almost all the sodium was released into solution and in this case the quantity of calcium is closed to the quantity of aluminum remaining in the gel (assuming the two charges of a Ca^{2+} can compensate two $[AlO_4]^-$ groups). Finally, in TAlCaZr-b, which has as little sodium as TAlCa-b but also includes zirconium, the quantity of Ca^{2+} remaining in the gel is sufficient to compensate both $[AlO_4]^-$ and $[ZrO_6]^{2-}$ groups.

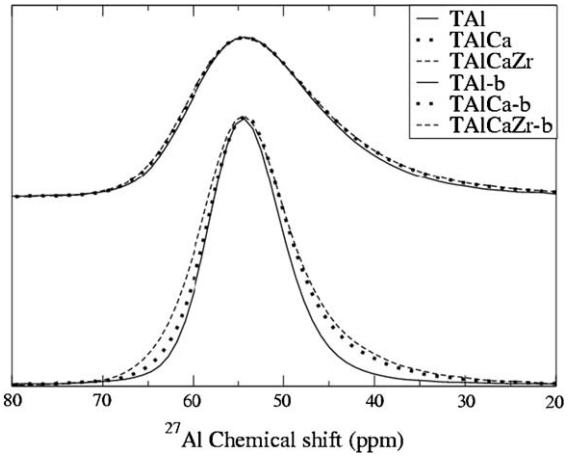

Fig. 11. ^{27}Al MAS spectra of pristine and basic-leached glasses.

The question now arises whether in the pristine TAlCa and TAlCaZr glasses aluminum is already compensated by Ca^{2+} or initially by Na^+ that is replaced by Ca^{2+} during leaching. In a study of aluminosilicate glasses with a series of alkali ions as charge-balancing cations (Dirken et al., 1995), a gradual increase was observed in the quadrupolar coupling constant with the increasing polarization power of the alkali ions (corresponding to the ratio z/r^2, where z is the valence and r is the atomic radius). To address this question with alkaline earths, two aluminosilicate glasses were fabricated, each containing a single type of possible charge-compensating cation: sodium (Na_2O–Al_2O_3–$3SiO_2$) or calcium ($2CaO$–Al_2O_3–$3SiO_2$). The ^{27}Al MAS spectra for these two glasses revealed that all the aluminum observable by NMR was in tetrahedral form. To detect the sensitivity of the ^{27}Al NMR parameters (isotropic chemical shift and quadrupolar interactions), two-dimensional multiple-quantum MAS (MQMAS) spectra were recorded to separate the contribution of the isotropic chemical shift and quadrupolar interaction to the broadening of the MAS NMR line. ^{27}Al 3QMAS spectra of these glasses were acquired at 78.6 MHz. Working at lower field (7.05 T instead of 11.7 T used for the MAS spectra in Fig. 11) more readily highlights the effect of the second order quadrupolar interaction. As shown by Fig. 12, when calcium exerts the charge-compensating role for the $[AlO_4]^-$ groups the site is significantly more extended, particularly with regard to the quadrupolar interaction. These results highlight the sensitivity of the ^{27}Al quadrupolar interaction with respect to the charge compensator and thus, the possibility of determining the nature of the aluminum charge compensation in

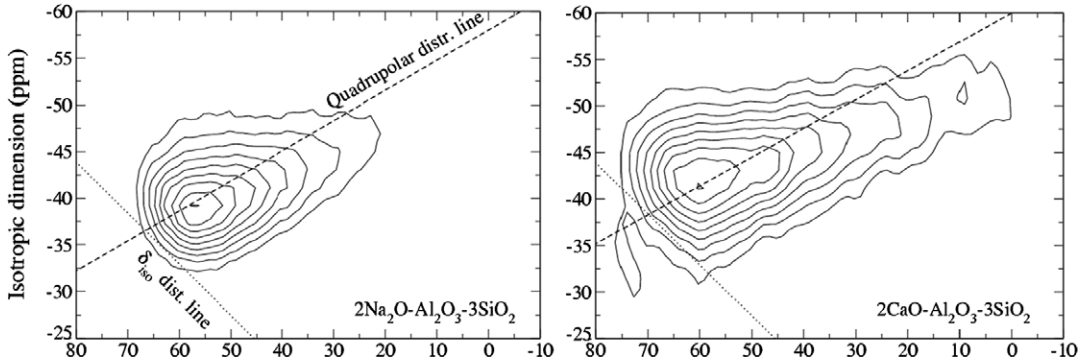

Fig. 12. ^{27}Al 3QMAS spectra (at 78.6 MHz) of $2CaO–Al_2O_3–3SiO_2$ and $Na_2O–Al_2O_3–3SiO_2$. Broken lines show the direction of the distributions of the second order quadrupolar interaction shift and of the isotropic chemical shift (δ_{iso}).

the event of competition between different cations. The minimal differences observed in the ^{27}Al MAS spectra of pristine glasses in this study (Fig. 11) suggest that the aluminum atoms have a similar environment, and thus that most of the aluminum is compensated by the same cation. Since this can only be sodium in TAl glass, which contains no calcium, and the TAlCa and TAlCaZr peaks are nearly superimposed on TAl, it can reasonably be assumed that $[AlO_4]^-$ charge compensation in all three glasses is ensured mainly by Na^+. The MQMAS data acquired on TAl-b and TAlCaZr-b gels after heating (Fig. 13) clearly show that the difference between the two spectra is due to an increase (in average) of the quadrupolar coupling constant. In light of the observations of the glasses on Fig. 12, this result confirms that calcium becomes the primary aluminum charge compensator in the gel rather than sodium. Under these conditions, sodium would be replaced by calcium around the aluminum during leaching.

Fig. 14 shows a ^{1}H–^{27}Al HETCOR spectrum of TAl-b. Two contributions of tetrahedral aluminum are resolved; along the proton dimension, the first one is near 0.5 ppm and the second one near 4 ppm. The two sites are separated by only a few *ppm* along the aluminum dimension, so that they cannot be resolved on a MAS-only spectrum as well as in MQMAS spectroscopy. These two proton resonances are clearly observed on the ^{1}H MAS spectra of heated TAl-b (Fig. 5a). The fact that the proton peak at about 1.6 ppm is not observed confirms its assignment to a silanol group. As in ^{1}H–^{29}Si HETCOR maps, these two contributions can represent a single aluminum species exchanging magnetization with different protons. However, slices along the aluminum dimension extracted at the two mean proton chemical shifts (0.5 and 4 ppm) show that they can be assigned to two different species. From ^{27}Al MAS spectra simulations obtained at very high field (17.6 T), Zeng et al. (2000) proposed two sites for aluminum; Al(Q^3)–OH site and Al(Q^4). Indeed Al(Q^3)–OH and Al(Q^4) should significantly differ in their cross-polarization

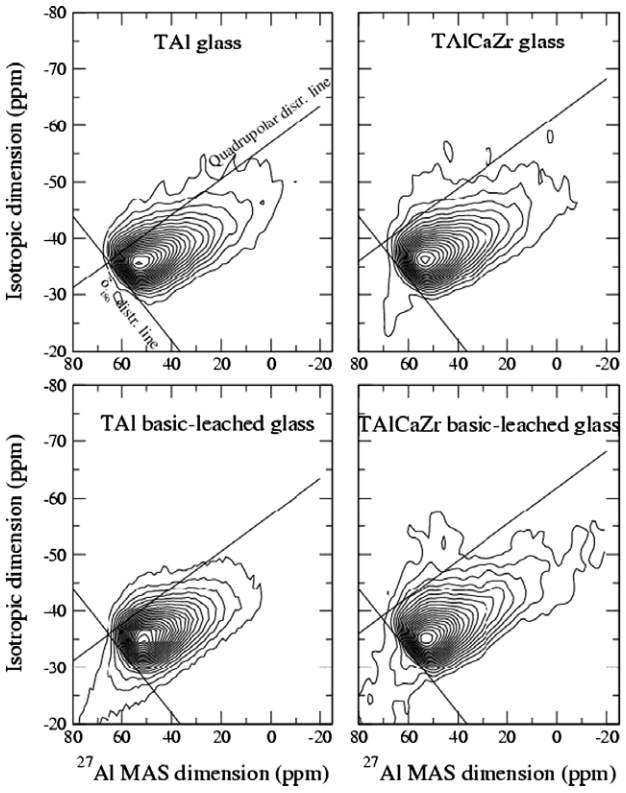

Fig. 13. ^{27}Al 3QMAS spectra (at 78.6 MHz) of TAl and TAlCaZr glasses and basic-leached glasses after heating for 60 h at 180 °C.

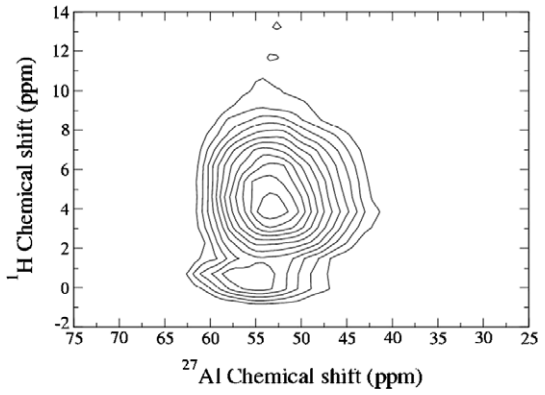

Fig. 14. ^{1}H → ^{27}Al HETCOR spectrum with 800 μs polarization time for TAl-b after heating for 60 h at 180 °C.

dynamics behaviors. MQHETCOR experiments (Amoureux and Pruski, 2002) will be conduced to address this question.

4. Conclusion

The purpose of this study was to determine how the gel structure can be influenced by the alteration solution and the glass composition. Very little work has focused to date directly on the structure of the alteration gels. This led us to investigate the potential of high-resolution solid-state NMR for probing the pristine glass and its evolution during leaching. This study concentrated on nuclei representative of the glass network generally encountered in silicate glasses, and generally present both in the glass and in the gel (^{29}Si and ^{27}Al). The proton and its coupling with neighboring nuclei were used to probe the leached glass. These NMR investigations could also be used in earth sciences for structural characterization of aluminosilicate melts, with some implications for natural magmatic systems interacting with water. NMR of ^{1}H correlated with other nuclei (^{1}H, ^{29}Si, and ^{27}Al) could inform about the speciation of water and its effect on the network depolymerization to elucidate the solubility and dissolution mechanisms of water in aluminosilicate melts and glasses. For example, ^{1}H–^{29}Si (or ^{1}H–^{27}Al) heteronuclear correlations can be used to discriminate silicon (or aluminum) species according to their proximity with different type of protons (OH, H_2O) in two-dimensional maps. Information about the nature of the charge-compensating cation of aluminum can also be obtained by ^{27}Al MQMAS from the sensitivity of the ^{27}Al quadrupolar interaction. Double-quanta NMR experiments may be very useful for identifying the proton species interacting with each other. This technique can also separate isolated Si–OH sites from those close to one another. These complementary methods represents very promising tools for extending our knowledge of hydrated aluminosilicates materials in relation with their physical properties.

Acknowledgments

The authors are grateful to two anonymous reviewers and to Associate Editor Bjorn O. Mysen for helpful comments that improved this manuscript.

Associate editor: Bjorn Mysen

References

Abraitis, P.K., Livens, F.R., Monteith, J.E., Small, J.S., Trivedi, D.P., Vaughan, D.J., Wogelius, R.A., 2000. The kinetics and mechanisms of simulated British Magnox waste glass dissolution as a function of pH, silicic acid activity and time in low temperature aqueous systems. *Appl. Geochem.* **15**, 1399–1416.

Advocat, T., Jollivet, P., Crovisier, J.L., Del Nero, M., 2001. Long-term alteration mechanisms in water for SON68 radioactive borosilicate glass. *J. Nucl. Mater.* **298**, 55–62.

Ai, X., Deng, F., Dong, J., Hu, W., Chen, L., Ye, C., 2002. Stability of layered sodium disilicate during hydration process as studied by multinuclear solid state NMR spectroscopy. *J. Phys. Chem. B* **106**, 9237–9244.

Ai, X., Deng, F., Dong, J., Hu, W., Xu, H., Ye, C., 2004. One- and two-dimensional solid-state magic angle spinning NMR studies on the hydration process of layered sodium disilicate SKS-6. *Solid State Nucl. Magn. Reson.* **25**, 216–226.

Amoureux, J.P., Fernandez, C., Steuernagel, S., 1996. Z filtering in MQMAS NMR. *J. Magn. Res. A* **123** (1), 116–118.

Amoureux, J.P., Pruski, M., 2002. Advances in MQMAS NMR. In: Grant, D.M., Harris, R.K. (Eds.), *Encyclopedia of Nuclear Magnetic Resonance*, vol. 9. J. Wiley, Chichester, pp. 226–251.

Angeli, F., Charpentier, T., Gin, S., Petit, J.C., 2001. ^{17}O 3Q-MAS NMR characterization of a sodium aluminoborosilicate glass and its alteration gel. *Chem. Phys. Lett.* **341**, 23–28.

Blet, V., Rudloff, D., Berne, P., Jollivet, P., Schweich, D., 2002. A systemic approach for the characterization of ion exchange in the altered layer of a non-radioactive nuclear glass. *Chem. Eng. Sci.* **57**, 3427–3438.

Bronniman, C.E., Zeigler, R.C., Maciel, G.E., 1988. Proton NMR study of dehydration of the silica gel surface. *J. Am. Chem. Soc.* **110** (7), 2023–2026.

Bunker, B.C., Tallant, D.R., Headley, T.J., Turner, G.L., Kirkpatrick, R.J., 1988. The structure of leached sodium borosilicate glass. *Phys. Chem. Glasses* **29**, 109–120.

Brunauer, S., Emmett, P.H., Teller, E., 1938. Adsorption of gases in multimolecular layers. *J. Am. Chem. Soc.* **60**, 309–319.

Carroll, S.A., Maxwell, R.S., Bourcier, W., Martin, S., Hulsey, S., 2002. Evaluation of silica-water surface chemistry using NMR spectroscopy. *Geochim. Cosmochim. Acta* **66**, 913–926.

Chuang, I.S., Kinney, D.R., Maciel, G.R., 1993. Interior hydroxyls of the silica gel system as studied by ^{29}Si CP-MAS NMR spectroscopy. *J. Am. Chem. Soc.* **115**, 8695–8705.

Chuang, I.S., Maciel, G.E., 1997. A detailed model of local structure and silanol hydrogen bonding of silica gel surfaces. *J. Phys. Chem.* **101**, 3052–3064.

Cody, G.D., Mysen, B.O., Lee, S.K., 2005. Structure vs. composition: a solid-state ^{1}H and ^{29}Si NMR study of quenched glasses along the Na_2O–SiO_2–H_2O join. *Geochim. Coscmochim. Acta* **69** (9), 2373–2384.

Delage, F., Ghaleb, D., Dussossoy, J.L., Chevallier, O., Vernaz, E., 1992. A mechanistic model for understanding nuclear waste glass dissolution. *J. Nucl. Mater.* **190**, 191–197.

Dirken, P.J., Nachtegaal, G.H., Kentgens, A.P.M., 1995. Off-resonance nutation nuclear magnetic resonance study of framework aluminosilicate glasses with Li, Na, K, Rb or Cs as charge-balancing cation. *Solid State Nucl. Magn. Reson.* **5**, 189–200.

El Rassy, H., Pierre, A.C., 2005. NMR and IR spectroscopy of silica aerogels with different hydrophobic characteristics. *J. Non Crystallogr. Solids* **351** (19–20), 1603–1610.

Engelhardt, G., Michel, D., 1987. *High-Resolution Solid-State NMR of Silicates and Zeolites*. John Wiley & Sons Ltd.

Feike, M., Demco, D.E., Graf, R., Gottwald, J., Hafner, S., Spiess, H.W., 1996. Broadband multiple-quantum NMR spectroscopy. *J. Magn. Res. A* **122**, 214–221.

Frydman, L., Harwood, J.S., 1995. Isotropic spectra of half-integer quadrupolar spins from bidimensional magic-angle-spinning NMR. *J. Am. Chem. Soc.* **117**, 5367–5368.

Galoisy, L., Pelegrin, E., Arrio, M.A., Ildefonse, P., Calas, G., 1999. Evidence for 6-coordinated zirconium in inactive nuclear waste glasses. *J. Am. Ceram. Soc.* **82** (8), 2219–2224.

Gin, S., 2000. Protective effect of the alteration gel: a key mechanism in the long-term behavior of nuclear waste glass. *Mater. Res. Soc. XXIV* **663**, 207–215.

Hamilton, J.P., Pantano, C.G., 1997. Effect of glass structure on the corrosion behavior of sodium-aluminosilicate glasses. *J. Non Crystallogr. Solids* **222**, 167–174.

Hamilton, J.P., Brantley, S.L., Pantano, C.G., Criscenti, L.J., Kubicki, J.D., 2001. Dissolution of nepheline, jadeite and albite glasses: toward

better models for aluminosilicate dissolution. *Geochim. Cosmochim. Acta* **65** (21), 3683–3702.

Jian Zhi, Hu, Ja Hun, Kwak, Herrera Jose, E., Yong, Wang, Peden Charles, H.F., 2005. Line narrowing in ^{1}H MAS spectrum of mesoporous silica by removing adsorbed H_2O using N_2. *Solid State Nucl. Magn. Res.* **27** (3), 200–205.

Kinsey, R.A., Kirkpatrick, R.J., Hower, J., Smith, K.A., Oldfield, E., 1985. High resolution aluminium-27 and silicon-29 nuclear magnetic resonance spectroscopic study of layer silicates, including clay minerals. *Am. Miner.* **70**, 537–548.

Klur, I., Jacquinot, J.F., Brunet, F., Charpentier, T., Virlet, J., Schneider, C., Tekely, P., 2000. NMR cross-polarization when T-IS > T-1 rho; examples from silica gel and calcium silicate hydrates. *J. Phys. Chem. B* **104** (44), 10162–10167.

Kohn, S.C., Dupree, R., Mortuza, M.G., 1992. The interaction between water and aluminosilicate magmas. *Chem. Geol.* **96**, 399–409.

Kohn, S.C., Dupree, R., Smith, M.E., 1989a. Proton environments and hydrogen-bonding in hydrous silicate glasses from proton NMR. *Nature* **337**, 539–541.

Kohn, S.C., Dupree, R., Smith, M.E., 1989b. A multinuclear magnetic resonance study of the structure of hydrous albite glasses. *Geochim. Coscmochim. Acta* **53**, 2925–2935.

Kümmerlen, J., Merwin, L.H., Sebald, A., Keppler, H., 1992. Structural role of H_2O in sodium silicate glasses: results from ^{29}Si and ^{1}H NMR spectroscopy. *J. Phys. Chem.* **96**, 6405–6410.

Liu, C.C., Maciel, G.E., 1996. The fumed silica surface: a study by NMR. *J. Am. Chem. Soc.* **118**, 5103–5119.

Maekawa, H., Maekawa, T., Kawamura, K., Yokokawa, T., 1991. The structural groups of alkali silicate glasses determined from ^{29}Si MAS-NMR. *J. Non Crystallogr. Solids* **127**, 53.

Maciel, G.E., Sindorf, D.W., 1980. Silicon-29 nuclear magnetic resonance study of the surface of silica gel by cross polarization and magic-angle spinning. *J. Am. Chem. Soc.* **102**, 7606–7607.

Massiot, D., Touzo, B., Trumeau, D., Coutures, J.P., Virlet, J., Florian, P., Grandinetti, P.J., 1996. Two-dimensional magic-angle spinning isotropic reconstruction sequences for quadrupolar nuclei. *Solid State Nucl. Magn. Reson.* **6**, 73–83.

Ménard, O., Advocat, T., Ambrosi, J.P., Michard, A., 1998. Behaviour of actinides (Th, U, Np and Pu) and rare earths (La, Ce and Nd) during aqueous leaching of nuclear glass under geological disposal conditions. *Appl. Geochem.* **13**, 105–126.

Muller, D., Gessner, W., Behrens, H.J., Scheler, G., 1981. Determination of the aluminium coordination in aluminium-oxygen compounds by solid-state high-resolution ^{27}AI NMR. *Chem. Phys. Lett.* **79**, 59.

Oestrike, R., Yang, W.H., Kirkpatrick, R.J., Hervig, R.L., Navrotsky, A., Montez, B., 1987. High-resolution ^{23}Na, ^{27}Al and ^{29}Si NMR spectroscopy of framework aluminosilicate glasses. *Geochim. Cosmochim. Acta* **51**, 2199–2209.

Oglesby, J.V., Zhao, P., Stebbins, J., 2002. Oxygen sites in hydrous aluminosilicate glasses: the role of Al–O–Al and H_2O. *Geochim. Cosmochim. Acta* **66**, 291–301.

Ollier, N., Concas, G., Panczer, G., Champagnon, B., Charpentier, T., 2003. Structural features of a Eu^{3+} doped nuclear glass and gels obtained from glass leaching. *J. Non Crystallogr. Solids* **328**, 207–214.

Padro, D., Schmidt, B.C., Dupree, R., 2003. Water solubility mechanism in hydrous aluminosilicate glasses: information from ^{27}Al MAS and MQMAS NMR. *Geochim. Coscmochim. Acta* **67** (8), 1543–1551.

Pelegrin, E., 2000. Étude comparée de la structure locale des produits d'altération du verre SON68 et de gels naturels, PhD thesis, University of Paris VII.

Robert, E., Whittington, A., Fayon, F., Pichavant, M., Massiot, D., 2001. Structural characterization of water-bearing silicate and aluminosilicate glasses by high-resolution solid-state NMR. *Chem. Geol.* **174**, 291–305.

Schaller, T., Sebald, A., 1995. One- and two-dimensional ^{1}H magic-angle spinning experiments on hydrous silicate glasses. *Solid State Nucl. Magn. Res.* **5**, 89–102.

Scheetz, B.E., Freeborn, W.P., Smith, D.K., Anderson, C., Zolensky, M., White, W.B., 1985. The role of boron in monitoring the leaching of borosilicate glass waste forms. *Sci. Basis Nucl. Waste Manage. VIII* **44**, 129–134.

Schmidt, B.C., Reimer, T., Kohn, S.C., Holtz, F., Dupree, R., 2001. Structural implications of water dissolution in haplogranitic glasses from NMR spectroscopy: influence of total water content and mixed alkali effect. *Geochim. Coscmochim. Acta* **65**, 2949–2964.

Smets, B.M.J., Lommen, T.P.A., 1982. The leaching of sodium aluminosilicate glasses studied by secondary ion mass spectrometry. *Phys. Chem. Glasses* **23**, 83.

Spalla, O., Barboux, P., Sicard, L., Lyonnard, S., Bley, F., 2004. Influence of insoluble elements on the nanostructure of water altered glasses. *J. Non Crystallogr. Solids* **347**, 56–68.

Tsomaia, N., Brantley, S.L., Hamilton, J.P., Pantano, C.G., Mueller, K.T., 2003. NMR evidence for formation of octahedral and tetrahedral Al and repolymerization of the Si network during dissolution of aluminosilicate glass and crystal. *Am. Mineralog.* **88**, 57–67.

Zeng, Q., Nekvasil, H., Grey, C.P., 1999. Proton environment in hydrous aluminosilicate glasses: a ^{1}H MAS, $^{1}H/^{27}Al$ and $^{1}H/^{23}Na$ TRAPDOR NMR study. *J. Phys. Chem. B* **103**, 7406–7415.

Zeng, Q., Nekvasil, H., Grey, C.P., 2000. In support of a depolymerization model for water in sodium aluminosilicate glasses: information from NMR spectroscopy. *Geochim. Cosmochim. Acta* **64**, 883–896.